Available online at www.sciencedirect.com
ScienceDirect
Journal of Sound and Vibration 306 (2007) 803–817
JOURNAL OF SOUND AND VIBRATION
www.elsevier.com/locate/jsvi

Detection and assessment of damage in 2D structures using measured modal response

Mohammad Reza Banan[a,b,*], Yousef Mehdi-pour[c]

[a]*Department of Civil Engineering, Shiraz University, Shiraz, Fars 7134851156, Iran*
[b]*Department of Civil Engineering, American University of Sharjah, UAE*
[c]*Civil Engineering Department, Islamic Azad University, Qeshm, Iran*

Received 26 August 2006; received in revised form 24 June 2007; accepted 27 June 2007

Abstract

Motivated by one of the concepts in the field of health monitoring for structural systems, a damage detection procedure is developed. In order to perform the system health monitoring, structural health along with sensor and actuator malfunction must be continuously checked. As a step toward developing a system health-monitoring scheme, this paper investigated structural damage detection, using a constrained eigenstructure assignment. The proposed damage detection method is constructed based on a concept of control theory and subspace rotation for two-dimensional (2D)-structural systems. To demonstrate the capabilities of the developed damage detection algorithm, the behavior of a simulated degraded braced-frame structure is studied. Using Monte Carlo simulation, the performance of the approach is evaluated. It shows that the proposed algorithm is potentially promising for application to real cases.

1. Introduction

During the lifetime of a structure sever damages might occur due to extreme events. Damage refers to a localized failure of a structural member. This failure can be a complete loss of some constitutive properties of the damaged member up to an unacceptable level. We assume this failure or degradation would primarily affect the stiffness properties. Therefore, it changes the modal characteristics of the dynamic response of the structure.

A well-designed structure may survive a damaging event but its safety cannot be generally guaranteed, based on the initial design, after such an experience. Undetected and unrepaired damage may lead to a structural failure requiring costly repair or loss of human lives. Therefore, it is essential to inspect any structure for damage, particularly after a severe loading event.

Visual inspection by an expert has been the only option available throughout most of structural monitoring history. But many parts of a structure might be difficult, if not impossible, to inspect visually. Therefore, using

*Corresponding author. Department of Civil Engineering, Shiraz University, Shiraz, Fars 7134851156, Iran.
E-mail addresses: banan@shirazu.ac.ir (MO.R. Banan), y.mehdipour@yahoo.com (Y. Mehdi-pour).

0022-460X/$ - see front matter © 2007 Elsevier Ltd. All rights reserved.
doi:10.1016/j.jsv.2007.06.026

Nomenclatures

$\mathbf{B}_0$	$n \times m$ control influence matrix
$\mathbf{C}$	$n \times n$ proportional damping matrix
$\mathbf{E}$	$r \times n$ output influence matrix
F	axial force
$\mathbf{G}$	$m \times r$ feedback gain matrix
$\mathbf{K}$	$n \times n$ stiffness matrix
$\mathbf{M}$	$n \times n$ mass matrix
M_1	member-end moment at node i
M_2	member-end moment at node j
$\mathbf{S}$	state vector
t_{ij}	amount of noise in mode i at the jth degree of freedom
$\mathbf{T}$	$3 \times n$ transformation matrix
$\mathbf{u}$	$m \times 1$ control force vector
$\mathbf{v}_i$	desired eigenvector
$\hat{\mathrm{v}}_i$	measured portion of $\mathbf{v}_i$
$\hat{\mathrm{v}}_i$	unmeasured portion of $\mathbf{v}_i$
$\tilde{\mathrm{v}}_{ij}$	jth member of the ith noisy mode shape
$\hat{\mathrm{v}}_{ij}$	jth member of the ith analytically mode shape
$\mathbf{x}$	$n \times 1$displacement vector
$\dot{\mathbf{x}}$	$n \times 1$ velocity vector
$\ddot{\mathbf{x}}$	$n \times 1$ acceleration vector
$\mathbf{z}$	$r \times 1$ output feedback variables
γ_{ij}	angle between two vectors
Δ	axial deformation
θ_1	member-end rotation at node i
θ_2	member-end rotation at node j
λ_i^d	desired eigenvalue
$\tilde{\lambda}_i$	ith noisy frequency
λ_i	ith analytical frequency

physical nondestructive testing to augment traditional inspection procedures has been increasingly viewed as a powerful alternative [1–3].

The ability to locate and assess damage in flexible structures has been significantly becoming important for improving the performance and life span of these systems. Many local or focused approaches have been developed and studied for the purpose of damage location and damage assessment, including X-ray, optical, infrared, and ultrasonic methods. Among global or system methods currently in development, those that use vibration responses and system identification, have considerably progressed in the last decades [4–6]. Here, system identification refers to the process that modifies or updates a finite element model of a structural system based on measuring response [7]. The motivation behind a system identification approach for damage detection is to quantify the damage information contained in the response as much and as effectively as possible [8].

Some researchers have been studying methods of structural damage locating using measured modal data [9–13]. These methods can be classified based on the definition of structural models and design parameters, utilization of the experimental data, and estimation of the parameters. Basically, these methods consider some sort of change. The change could be frequency, mode shape, energy, and stiffness or flexibility. In general, the majority of these methods can be classified as model update methods, which are (1) optimal up-date matrix methods, (2) sensitivity methods, (3) control-based eigenstructure assignment techniques, and (4) hybrid methods [4].

If we were to describe few methods from each of the four classes, this would require a lengthy paper, which is out of the scope of our objective. Therefore, we just focus on the methods of class 3. These methods are based on the concept of control [14–16].

Designers of control systems have traditionally used eigenstructure assignment techniques to force a system to respond in a predetermined way. For model refinement and damage locating, the desired eigenstructure, i.e., eigenvalues and eigenvectors, is the response that is measured in the test. In 1988, Minas and Inman [17] and in 1990, Zimmerman and Widengren [18] derived methods that determine the pseudo (fictitious) controller required to produce test eigenstructures. The control gains can then be translated into matrix adjustments applied to the initial finite element model. Zimmerman and Kaouk [15] in 1992 applied this eigenstructure model refinement algorithm to structural damage detection techniques. A major difficulty associated with their approach is that the method identifies matrix coefficients changes and thus requires an additional step of identifying structural members corresponding to these changes. This additional step is not a straightforward step for complex structures. Besides, the method requires a solution of the generalized algebraic Riccati equation. The authors proposed an iterative solution to preserve the load path of the undamaged structure,

i.e., to maintain the zero–nonzero pattern of the undamaged stiffness matrix. But when a structural member is completely damaged, the initial load path is broken. Consequently, for damage cases where the stiffness of a member is completely lost, preserving the load path is not valid anymore.

Basically, to perform successfully system health monitoring, structural health along with sensor and actuator malfunctioning must be monitored. So, in 1994, Lim [14] proposed a structural damage detection method using a constrained eigenstructure assignment. His approach might be used not only for structural damage detection (partial and complete loss of stiffness) but also for sensor monitoring and actuator performance in a unified manner. Besides, the additional step of correlating matrix coefficient changes to structural parameter changes is avoided. The proposed approach requires neither a solution of Riccati equation nor any iteration to converge to a solution.

To demonstrate capabilities of any newly proposed approach, the authors usually use either truss or mass–spring systems. Studying the performance of these damage detection methods when applied to other structural system such as frames are not usually discussed.

In this paper, we focus on damage detection process for two-dimensional (2D) structures. Damage is defined as the loss of stiffness in a single member of 2D-structural systems. We will follow the formulation of the eigenstructure assignment for 2D trusses developed by Lim [14] and derive the appropriate relations for frame structures and propose an algorithm. The algorithm uses incomplete measured modal testing data. It has the capability of locating and assessing both complete and partial damages. Finally, the identification limitations of the proposed method are discussed.

2. Problem formulation

The proposed algorithm consists of two major steps. In the first step, we use subspace rotation technique to determine the location of damage. In the second step, we employ some well-defined concepts in the field of control to assess the magnitude of identified damage. These steps are briefly discussed here.

2.1. Damage location

Consider a finite element model of a structure with n degrees of freedom and a feedback control system

$$\mathbf{M}\ddot{\mathbf{x}} + \mathbf{C}\dot{\mathbf{x}} + \mathbf{K}\mathbf{x} = \mathbf{B}_0\mathbf{u} \tag{1}$$

where $\mathbf{M}$, $\mathbf{C}$, and $\mathbf{K}$ are $n \times n$ analytical mass, damping, and stiffness matrices, respectively, $\mathbf{x}$ is an $n \times 1$ vector of displacements, $\mathbf{B}_0$ that defines the locations of control forces is an $n \times m$ control influence matrix, $\mathbf{u}$ is $m \times 1$ vector of control forces, and the over dots represent differentiation with respect to time. In addition, the $r \times 1$ output vector $\mathbf{z}$ of sensor measurements is given by

$$\mathbf{z} = \mathbf{E}\mathbf{x}, \tag{2}$$

where $\mathbf{E}$ is an $r \times n$ output influence matrix. The employed control law is a general linear output feedback represented as follows:

$$\mathbf{u} = -\mathbf{G}\mathbf{z}, \tag{3}$$

where $\mathbf{G}$ is the $m \times r$ feedback gain matrix. In 1983, Andry et al. [18] proved that if a system described by Eqs. (1) and (2) is controllable and observable, then by proper selection of $\mathbf{G}$, $\max(m, r)$ closed-loop (controlled) eigenvalues can be assigned. This maximum number of eigenvalues which is $\max(m, r)$ closed-loop eigenvectors can be partially assigned with $\min(m, r)$ entries in each eigenvector being arbitrarily assigned. Vector $\mathbf{z}$ contains output feedback variables. This vector consists of relative measured displacements as follows:

$$\mathbf{z} \equiv \mathbf{d} = \mathbf{B}_0^{\mathrm{T}}\mathbf{x}, \tag{4}$$

where $\mathbf{d}$ is vector of relative displacements. From Eqs. (3) and (4), the control force becomes

$$\mathbf{u} = -\mathbf{G}\mathbf{B}_0^{\mathrm{T}}\mathbf{x}. \tag{5}$$

Assume the changes in mass and damping properties due to damage are not significant. Then, substitute the control force into the equation of motion, Eq. (1), and rearranging it. We will have

$$\mathbf{M}\ddot{\mathbf{x}} + \mathbf{C}\dot{\mathbf{x}} + (\mathbf{K} + \mathbf{B}_0\mathbf{G}\mathbf{B}_0^{\mathrm{T}})\mathbf{x} = \mathbf{0}. \tag{6}$$

In this equation term, $\mathbf{B}_0\ \mathbf{G}\ \mathbf{B}_0^{\mathrm{T}}$ is a perturbation term that is generated due to the loss of stiffness. It shows that the stiffness of the system is modified. Redistribution of the gain matrix to appropriate element degrees of freedom is performed by matrix $\mathbf{B}_0$.

Now, let us to define our desired eigenvalue and eigenvector λ_i^d and $\mathbf{v}_i^d$, respectively. Then the eigenvalue problem associated with Eq. (6) will be as follows:

$$\left[\mathbf{M}\lambda_i^{d^2} + \mathbf{D}\lambda_i^d + (\mathbf{K} + \mathbf{B}_0\mathbf{G}\mathbf{B}_0^{\mathrm{T}})\right]\mathbf{v}_i^d = 0. \tag{7}$$

To demonstrate the feasibility of the procedure we employ a simple element. Fig. 1 illustrates an element with prescribed degrees of freedom and nodal forces. The relationship between nodal deformations and nodal forces for this element is as follows:

$$\begin{Bmatrix} F \\ M_1 \\ M_2 \end{Bmatrix} = \begin{bmatrix} \dfrac{\mathrm{EA}}{L} & 0 & 0 \\ 0 & \dfrac{4\,\mathrm{EI}}{L} & \dfrac{2\,\mathrm{EI}}{L} \\ 0 & \dfrac{2\,\mathrm{EI}}{L} & \dfrac{4\,\mathrm{EI}}{L} \end{bmatrix} \begin{Bmatrix} \Delta \\ \theta_1 \\ \theta_2 \end{Bmatrix}. \tag{8}$$

If constitutive properties or axial and flexural stiffnesses of each element are presented by $g_1 = \mathrm{EA}/L$ and $g_2 = \mathrm{EI}/L$, then Eq. (8) turns to

$$\begin{Bmatrix} F \\ M_1 \\ M_2 \end{Bmatrix} = \begin{bmatrix} g_1 & 0 & 0 \\ 0 & 4g_2 & 2g_2 \\ 0 & 2g_2 & 4g_2 \end{bmatrix} \begin{Bmatrix} \Delta \\ \theta_1 \\ \theta_2 \end{Bmatrix}. \tag{9}$$

This equation can be written in the following form:

$$\mathbf{u}_j = \mathbf{G}_j\mathbf{d}_j. \tag{10}$$

Assuming linear behavior for geometry and constitutive material of the structure, $\mathbf{G}_j$ can be decomposed in the following form:

$$\begin{bmatrix} g_1 & 0 & 0 \\ 0 & 4g_2 & 2g_2 \\ 0 & 2g_2 & 4g_2 \end{bmatrix} = g_1 \begin{bmatrix} 1 & 0 & 0 \\ 0 & 0 & 0 \\ 0 & 0 & 0 \end{bmatrix} + g_2 \begin{bmatrix} 0 & 0 & 0 \\ 0 & 4 & 2 \\ 0 & 2 & 4 \end{bmatrix}. \tag{11}$$

Eq. (11) can be written in matrix form as

$$\mathbf{G}_j = g_{1j}\mathbf{D}_1 + g_{2j}\mathbf{D}_2. \tag{12}$$

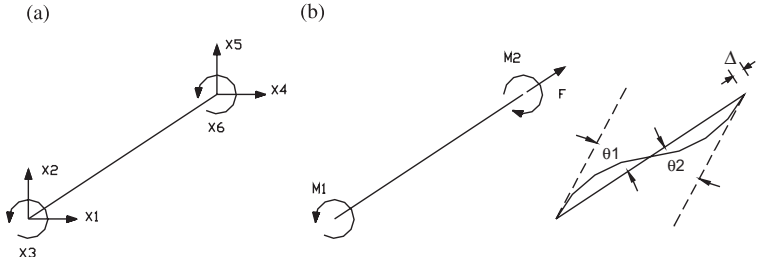

Fig. 1. (a) Global nodal displacements, (b) effective forces and self-straining deformations.

The subscript j represents that this relation is derived for the jth member of the structure. On the other hand, the relation between deformations and nodal displacements of the jth element in global coordinate system is as follows [19]:

$$\mathbf{d}_j = \mathbf{B}_{0j}\mathbf{x}. \tag{13}$$

In this equation, $\mathbf{x}$ is the vector of nodal displacements in global coordinate system and $\mathbf{d}_j$ and the transformation matrix $\mathbf{B}_{0j}$ are defined as

$$\mathbf{d}_j = \begin{Bmatrix} \Delta \\ \theta_1 \\ \theta_2 \end{Bmatrix}, \quad \mathbf{B}_{0j} = \begin{bmatrix} 0 & \cdots & 0 & -C & -S & 0 & 0 & \cdots & 0 & C & S & 0 & 0 & \cdots & 0 \\ 0 & \cdots & 0 & -S & C & L & 0 & \cdots & 0 & S & -C & 0 & 0 & \cdots & 0 \\ 0 & \cdots & 0 & -S & C & 0 & 0 & \cdots & 0 & S & -C & L & 0 & \cdots & 0 \end{bmatrix}, \tag{14}$$

where $C = \cos\phi$, $S = \sin\phi$ and ϕ is the orientation of the jth element relative to the global coordinate system. From Eqs. (9) and (13), we will have

$$\mathbf{u}_j = \mathbf{G}_j\mathbf{B}_{0j}\mathbf{x}, \tag{15}$$

where $\mathbf{u}_j$ is the vector of control force which is enforced on the jth element.

Now, consider Eq. (7) and by rearranging it, define $\mathbf{v}_i^d$ as follows:

$$\mathbf{v}_i^d = -(\mathbf{M}\lambda_i^{d^2} + \mathbf{D}\lambda_i^d + \mathbf{K})^{-1}\mathbf{B}_{0j}\,\mathbf{G}_j\,\mathbf{B}_{0j}^{\mathrm{T}}\,\mathbf{v}_i^d. \tag{16}$$

By substituting Eq. (12) in Eq. (16) the following relation yields

$$\mathbf{v}_i^d = -(\mathbf{M}\lambda_i^{d^2} + \mathbf{D}\lambda_i^d + \mathbf{K})^{-1}\left\{g_{1j}\mathbf{B}_{0j}\mathbf{D}_1\mathbf{B}_{0j}^{\mathrm{T}} + g_{2j}\mathbf{B}_{0j}\mathbf{D}_2\mathbf{B}_{0j}^{\mathrm{T}}\right\}\mathbf{v}_i^d. \tag{17}$$

Let us define $\mathbf{P}^a{}_{ij}$ and $\mathbf{P}^b{}_{ij}$ as follows:

$$\mathbf{P}_{ij}^a = -(\mathbf{M}\lambda_i^{d^2} + \mathbf{D}\lambda_i^d + \mathbf{K})^{-1}\mathbf{B}_{0j}\mathbf{D}_1\mathbf{B}_{0j}^{\mathrm{T}}, \tag{18}$$

$$\mathbf{P}_{ij}^b = -(\mathbf{M}\lambda_i^{d^2} + \mathbf{D}\lambda_i^d + \mathbf{K})^{-1}\mathbf{B}_{0j}\mathbf{D}_2\mathbf{B}_{0j}^{\mathrm{T}}. \tag{19}$$

Then Eq. (17) can be expressed by

$$\mathbf{v}_i^d = \mathbf{P}_{ij}^a\alpha_{ij} + \mathbf{P}_{ij}^b\beta_{ij}, \tag{20}$$

where $\alpha_{ij} = g_{1j}\mathbf{v}_i^d$ and $\beta_{ij} = g_{2j}\mathbf{v}_i^d$. This equation shows that $\mathbf{v}_i^d$ is a linear combination of vectors $\mathbf{P}^a{}_{ij}$ and $\mathbf{P}^b{}_{ij}$ that span a subspace which contains $\mathbf{v}_i^d$. But due to errors in modeling and measurements, the desired eigenvector might not precisely locate in this subspace. If so, the closest possible eigenvector to $\mathbf{v}_i^d$ can be compute in a least-squares sense as follows:

$$\mathbf{v}_{ij}^a = \mathbf{P}_{ij}\mathbf{P}_{ij}^+\mathbf{v}_i^d \tag{21}$$

where $\mathbf{v}_{ij}^a$ is the best achievable eigenvector and $\mathbf{P}_{ij}$ and $\mathbf{P}_{ij}^+$ are defined in the following equation:

$$\mathbf{P}_{ij} = \begin{bmatrix} \mathbf{P}_{ij}^a & \mathbf{P}_{ij}^b \end{bmatrix} \quad \text{and} \quad \mathbf{P}_{ij}^+ = (\mathbf{P}_{ij}^{\mathrm{T}}\mathbf{P}_{ij})^{-1}\mathbf{P}_{ij}^{\mathrm{T}}. \tag{22}$$

The relationship between the vectors $\mathbf{v}_{ij}^a$ and $\mathbf{v}_i^d$ as well as the subspace spanned by the columns of $\mathbf{P}^a{}_{ij}$ and $\mathbf{P}^b{}_{ij}$ are illustrated in Fig. 2. If the jth structural member is damaged then $\mathbf{v}_i^d$ lies in the shown subspace and $\mathbf{v}_{ij}^a$ and $\mathbf{v}_i^d$ will be identical. These two vectors will not be identical if either mode i is not significantly affected by the damage developed in member j or other members might be damaged.

By computing $\mathbf{v}_{ij}^a$ and its angle with $\mathbf{v}_i^d$ for all structural members, one can spot the damaged element. Based on this concept, the element for which the angle between these two vectors is either zero or smaller than other values could be the most probable damaged element. The angle between these two vectors can be computed as

$$\gamma_{ij} = \frac{180}{\pi}\cos^{-1}\left(\frac{\mathbf{v}_{ij}^{a\mathrm{T}}\mathbf{v}_i^d}{\left\|\mathbf{v}_{ij}^a\right\|_{\mathrm{F}}\left\|\mathbf{v}_{\mathrm{i}}^d\right\|_{\mathrm{F}}}\right). \tag{23}$$

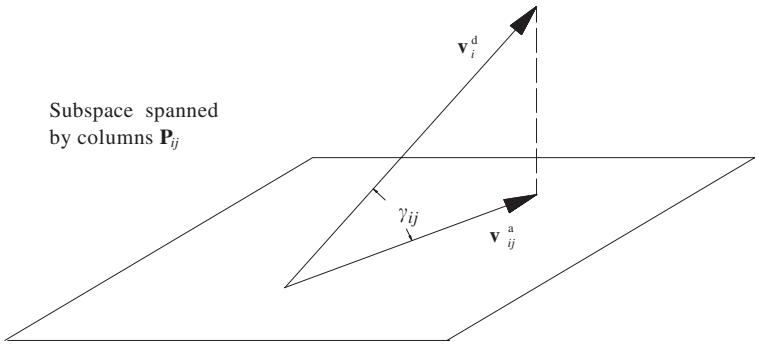

Fig. 2. Relation between two vectors.

But, the vector of measurements is usually incomplete. It is because of (i) limited number of sensors, (ii) hard to reach some parts of structures, and (iii) some degrees of freedom could not be measured. Therefore, the eigenvectors are incomplete. We partition the desired eigenvector into two parts as follows:

$$\mathbf{v}_i^d = \begin{Bmatrix} \hat{\mathbf{v}}_i \\ \bar{\mathbf{v}}_i \end{Bmatrix}, \tag{24}$$

where $\hat{\mathbf{v}}_i$ is the measured part and $\bar{\mathbf{v}}_i$ is the unmeasured portion of desired eigenvector. Using Eq. (21), the best achievable eigenvector is defined as

$$\hat{\mathbf{v}}_{ij}^a = \mathbf{P}_{ij}\hat{\boldsymbol{P}}_{ij}^{+}\hat{\mathbf{v}}_i, \tag{25}$$

where $\hat{\boldsymbol{P}}_{ij}^{+}$ contains the rows corresponding to $\hat{\mathbf{v}}_i$. The angle defined in Eq. (23) becomes as follows:

$$\hat{\gamma}_{ij} = \frac{180}{\pi}\cos^{-1}\left(\frac{\tilde{\mathbf{v}}_{ij}^{a\mathrm{T}}\hat{\mathbf{v}}_i^d}{\left\|\tilde{\mathbf{v}}_{ij}^a\right\|_{\mathrm{F}}\left\|\hat{\mathbf{v}}_i^d\right\|_{\mathrm{F}}}\right), \tag{26}$$

where $\tilde{\mathbf{v}}_{ij}^a$ is that partition of vector $\hat{\mathbf{v}}_{ij}^a$ which is corresponding to the measured part of the desired eigenvector $\hat{\mathbf{v}}_i$.

The main advantages of using the best achievable eigenvector concept proposed by Lim [20] could be summarized as follows. First, it allows partial specification of the eigenvector and second the measurement errors that are not consistent with the analytical model are filtered out.

2.2. Magnitude of damage

After identification of damaged members the eigenstructure assignment is employed to compute the magnitude of damage. Using state-space, the equation of motion (1) becomes as

$$\dot{\mathbf{S}} = \mathbf{A}\mathbf{S} + \mathbf{B}\hat{\mathbf{u}}, \tag{27}$$

where in this equation matrices $\mathbf{A}$, $\mathbf{B}$, and $\mathbf{S}$ are defined as follows:

$$\mathbf{A} = \begin{bmatrix} \mathbf{0} & \mathbf{I} \\ -\mathbf{M}^{-1}\mathbf{K} & -\mathbf{M}^{-1}\mathbf{C} \end{bmatrix}, \quad \mathbf{B} = \begin{bmatrix} \mathbf{0} \\ \mathbf{M}^{-1}\hat{\mathbf{B}}_0 \end{bmatrix}, \quad \mathbf{S} = \begin{Bmatrix} \mathbf{x} \\ \dot{\mathbf{x}} \end{Bmatrix}, \tag{28}$$

Matrix $\hat{\mathbf{B}}_0$ contains only those columns corresponding to the damaged members. The output Eq. (2) then becomes

$$\hat{\boldsymbol{z}} = \mathbf{E}\mathbf{S} = \begin{bmatrix} \hat{\mathbf{B}}_0^{\mathrm{T}} & \mathbf{0} \end{bmatrix}\mathbf{S}. \tag{29}$$

The output feedback is thus defined as

$$\hat{\mathbf{u}} = -\mathbf{G}\hat{\mathbf{z}} = -\mathbf{GES}. \tag{30}$$

Now we have to find the diagonal gain matrix $\mathbf{G}$. The best achievable eigenvectors are given by Eq. (21) and the desired eigenvalues and eigenvectors are as follows:

$$\mathbf{v}_{ia} = \mathbf{P}_i \hat{\mathbf{P}}_i^{+} \mathbf{v}_i, \tag{31}$$

where $\mathbf{P}_i = (\lambda_i^d \mathbf{I} - \mathbf{A})^{-1}\mathbf{B}$ and $\hat{\mathbf{P}}_i^{+}$ contains rows of the upper-half of $\mathbf{P}_i$ corresponding to the measured degrees of freedom used in $\mathbf{v}_i$ [14]. Using the constrained eigenstructure assignment algorithm by Andry et al. [18], the jth diagonal gain of $\mathbf{G}$ is computed as

$$\mathbf{g}_j = -\mathbf{\Psi}_j \mathbf{\Omega}_j^{+\mathrm{T}}, \tag{32}$$

where $\mathbf{g}_j$ is the vector of stiffness parameters changes of the jth structural member, $\mathbf{\Psi}j$ is the jth row of $\mathbf{\Psi}$ and $\mathbf{\Omega}_j$ is the jth row of $\mathbf{\Omega}$. In the above equation, the matrices $\mathbf{\Psi}$ and $\mathbf{\Omega}$ are defined as

$$\begin{aligned} \mathbf{\Omega} &\equiv \hat{\mathbf{E}}\,\mathbf{V}, \\ \mathbf{\Psi} &\equiv \mathbf{Y} - \mathbf{A}_1\mathbf{V}, \end{aligned} \tag{33}$$

where $\hat{\mathbf{E}}$, $\mathbf{A}_1$, $\mathbf{Y}$, and $\mathbf{V}$ are defined as follows [12]:

$$\begin{aligned} &\hat{\mathbf{A}} = \mathbf{T}^{-1}\mathbf{A}\mathbf{T} = \begin{bmatrix} \mathbf{A}_1 \\ \mathbf{A}_2 \end{bmatrix}, && \hat{\mathbf{B}} = \mathbf{T}^{-1}\mathbf{B} = \begin{bmatrix} \mathbf{I}_m \\ \mathbf{0} \end{bmatrix}, && \hat{\boldsymbol{E}} = \mathbf{E}\mathbf{T}, \\ &\mathbf{V} = \mathbf{T}^{-1}\mathbf{W}, && \mathbf{Y} = \mathbf{S_1}\mathbf{W}\boldsymbol{\Lambda}, \\ &\mathbf{W} = \begin{bmatrix} \mathbf{v}_{1a} & \mathbf{v}_{2a} & \cdots & \mathbf{v}_{pa} \end{bmatrix}, && \boldsymbol{\Lambda} = \mathrm{diag}(\lambda_1, \lambda_2, \ldots, \lambda_p), && \mathbf{T}^{-1} = \begin{bmatrix} \mathbf{S}_1 \\ \mathbf{S}_2 \end{bmatrix}. \end{aligned} \tag{34}$$

Derivation of Eq. (33) corresponds to the stiffness parameter changes of the jth structural member, i.e., the magnitude of structural damage that satisfies the measured eigenvalues and eigenvectors in the least-squares sense. Owing to inaccuracy (noise) in measured modes and the analytical model, the magnitude of structural damage will not be exact.

2.3. Identification limitation

For calculation of $\hat{\mathbf{P}}_{ij}^{+}$ in Eq. (24) the following constraint must be satisfied

$$\mathrm{rank}(\hat{\mathbf{P}}_{ij}) \leqslant N\,\mathrm{sens} \leqslant N\,\mathrm{dof},$$

where Nsens is the number of sensors and Ndof is the number of degrees of freedom of the finite element model of the structure. Thus, number of rows of matrix $\hat{\mathbf{P}}_{ij}$ is equal to number of placed sensors. The number of columns of this matrix is equal to 12 (refer to definition of $\mathbf{P}_{ij}$). A frame element with six degrees of freedom has three independent degrees of freedom. Therefore, $\mathbf{P}_{ij}$ have maximum three independent columns. Consequently, the maximum rank of $\hat{\mathbf{P}}_{ij}$ will be three. It is necessary to say that if $\mathbf{P}_{ij}$ is constructed for the frame element where one end is hinge and the other end is clamped, the rank of matrix $\hat{\mathbf{P}}_{ij}$ is less than three. The relationship between the minimum number of placed sensors and rank of the matrix $\hat{\mathbf{P}}_{ij}$ is as

$$\min(\mathrm{rank}(\hat{\mathbf{P}}_{ij}), 3) \leqslant N\,\mathrm{sens} \leqslant N\,\mathrm{dof}.$$

2.4. Operational modal analysis

The success of the proposed algorithm depends on the quality of the modal data of the structure under investigation. Obtaining relatively accurate modal vectors and natural frequencies, for a complex structure,

from real noisy and sparse measurements is not a simple task but can be achieved. It has been an active field of research especially during past four decades. While it is not the objective of this paper we address some issues in this regard.

Extracting modal parameters (natural frequencies, damping loss factors and modal constants) from measured vibration data can be deduced by modal analysis. Based on the measured data, which can be in the form of either impulse responses or frequency response functions, modal analysis can be categorized as time domain modal analysis and frequency domain modal analysis. Some of the well-known methods in each of these categories are as follows. In time domain one might use least-squares time-domain method, Ibrahim time-domain method, random decrement method, ARMA time-series method, least-squares complex exponential method. Some of the methods in frequency domain are least-square method, peak-picking method, Dobson's method, circle fit method, and inverse FRF method [21–23].

Many researches namely Ibrahim and Mikulcik [24], Jauang and Papa [25], Brown et al. [26], James et al. [27], Hermans and Van der Auweraer [28], Parloo et al. [29] and Brincker and Andersen [30], in their works have already addressed different methods for deducing modal parameters from experimental data. More recently, Mohanty and Rixen [31] proposed a procedure for identifying mode shapes and modal frequencies in the presence of both noise and unknown harmonic excitation.

In this paper, our intention is developing an algorithm and numerically studying its behavior. Exposing the algorithm to real data is beyond the scope of this paper. Therefor, in the next section, we will try to show the capabilities of the developed algorithm in a simulation environment.

3. Numerical studies

In this section, we investigate the performance of this devised approach through numerical simulation implemented to a braced-frame structure. In a numerical simulation environment, the behavior of the developed damage detection algorithm is studied with respect to change in some parameters such as location and extension of damage, sensor placement in view of number and location, and magnitude of error in measuring data.

The topological characteristic of the desired structure is illustrated in Fig. 3. This structure is made of steel frame and truss elements with rigid beam–column connections (moment resisting frame) and simple bracing connection to the joints. The Young's modulus of steel is $2\times10^{6}\,\mathrm{kg\,C\,m^{-2}}$ and the other properties of structural members are presented in Table 1.

To create the real condition of measuring process in a modal experiment through a simulation environment, we have to consider a few factors that will affect the quality of measurements and consequently the output of the proposed damage identification algorithm. So, the employed simulated model has the following features.

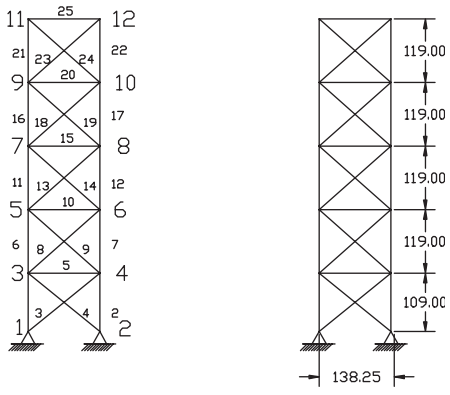

Fig. 3. Case study: braced frame.

Table 1
Properties of elements

Element type	Area (cm^2)	I (cm^4)	ρ ($kg\,cm^{-1}$)
Bracing	15	0	0.15
Beam	15	100	0.15
Column	30	100	0.30

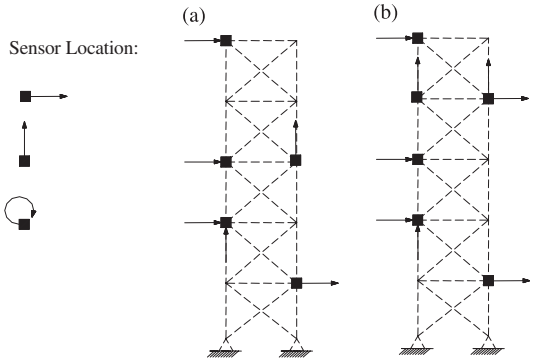

Fig. 4. Two cases of sensor placement: (a) 6 sensors and (b) 8 sensors.

3.1. Damage in the finite element model of the structure

We have assumed that the damage due to a destructive event is developed as stiffness reduction in a member. It means that the changes in other constitutive parameters of the member, such as mass and damping, are not significant. So, the damage in the model of the structure is considered by stiffness reduction of a desired member. In this study, we introduce damage rates in three different levels of 25%, 50%, and 95% in a specified element.

3.2. Measured data

Owing to noise in the measured modal data (natural frequencies and mode shapes), sensor placement difficulties and limited number of sensors, the measured data is noisy and sparse. In the simulation environment we have separately considered these two realistic features of the measured data.

(*i*) *Sparsity simulation*: It is almost impossible to measure all components of displacements at all degrees of freedom of a real structure. So, the measurements are incomplete in space, which causes the sparsity of data. We partition each analytical eigenvector $\mathbf{v}_i$ to two parts; one corresponds to the measured degrees of freedom, $\hat{\mathbf{v}}_i$ and the other corresponds to the unmeasured degrees of freedom $\bar{\mathbf{v}}_i$. Next, we disregard the unmeasured portion of each eigenvector $\bar{\mathbf{v}}_i$ and reduce the size of each eigenvector to the size of measured degrees of freedom $\hat{\mathbf{v}}_i$. In Fig. 4, locations of instrumented sensors, which are mounted on the structure are shown. These sensors measure only translational degrees of freedom.

(ii) *Noise simulation*: Noise in the measured data is not systematic, it has a random nature. We consider the effect of white noise on the measured data, by employing the following relation:

$$\tilde{\lambda}_i = \lambda_i(1 + t_{i0}), \quad \tilde{\mathbf{v}}_{ij} = \hat{\mathbf{v}}_{ij}(1 + t_{ij}), \tag{35}$$

where $\tilde{\lambda}_i$ and $\tilde{\mathbf{v}}_i$ are noisy modal data, λ_i and $\hat{\mathbf{v}}_i$ are analytically modal data and t_{ij} is amount of noise which is generated by a random number generator. Index i is mode number and index j is the component number of each eigenvector.

3.3. Conducting a modal experiment

Monte Carlo simulation is used to study the behavior of the proposed damage detection algorithm on a desired structure. We excite the structure in its first six vibrational modes. In each mode, the algorithm is run 10 times and the results of detection process are recorded. After 60 times running the detection process for each damage scenario, we attain relatively enough statistical information about the performance of this algorithm and will be able to evaluate the abilities of the devised approach.

3.4. Damage cases

The parameters that characterize the damage cases consist of the number and locations of sensors, rate of damage, and the amount of error in the measured data. By considering different values for each of these parameters, we can construct different damage scenarios. For illustrative purpose, we consider the symmetric structure shown in Fig. 3. Some of the studied damage cases for this structure are given in Table 2.

We assume that the damage may occur at only one member of half of the structure (because of symmetry) at once. In order to study the sensitivity of the developed algorithm to the location of damage, we have to apply a fixed value for a desired damage case to each element of the structure.

4. Damage detection criterion

By computing the angle between each mode shape vector and its correspond achievable eigenvector for each member of the structure and searching for the minimum value of these computed angles, the location of damage member is determined.

Table 2
Damage scenarios

Parameter	Corresponding value(s)
Number of sensors	6 and 8
Damage (%)	25, 50, and 95
Error (%)	1, 5, 10, and 20

Table 3
A typical damage case

Damaged element	9
Error in measurements	5%
Number of sensors	6
Locations of sensors (dof)	4-16-17-19-25-26
Damage condition	Strut out

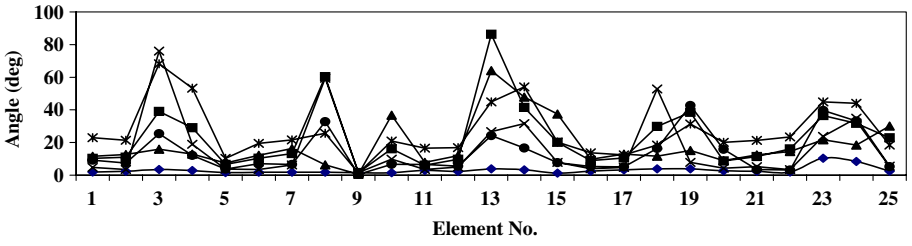

Fig. 5. Results of damage detection process for considered typical case (5% of error and 6 sensors). Mode 1: —◆—, Mode 2: —■—, Mode 3: —▲—, Mode 4: —×—, Mode 5: —✳—, Mode 6: —●—.

To demonstrate the approach of detection process, we first simulate a damage case, described in Table 3. Then by implying the detection algorithm, we will try to find the damaged member.

Fig. 5 summarized the results of the damage detection process. We have used first six vibration modes of the damaged structure that is created by simulation. In this figure, the horizontal axis is element number and the vertical axis represents the angle between each mode shape vector and the corresponding achievable eigenvector for an element [14]. One can observe that the trend of detection curves leads to element number 9.

In simulation environment, one can generate different damage cases. For each damage case the damage detection algorithm follows the above-mentioned detection process, to determine the desired case.

5. Numerical results

Figs. 6–8 show the results of the simulation study. Each figure represents the effects of; number of sensors, rate of damage and rate of error in the measured data on the detection of damage location. The horizontal axis gives the story number associated to the damaged member and the vertical axis gives the number of successfully detected damage location. For each damaged element with fixed amounts of damage and error we simulate 10 different sets of the first six eigenvectors, which are measured at either 6 or 8 degrees of freedom. Since we consider 10 sets of the first six incomplete eigenvectors, the number of runs of damage detection process for each element is 60.

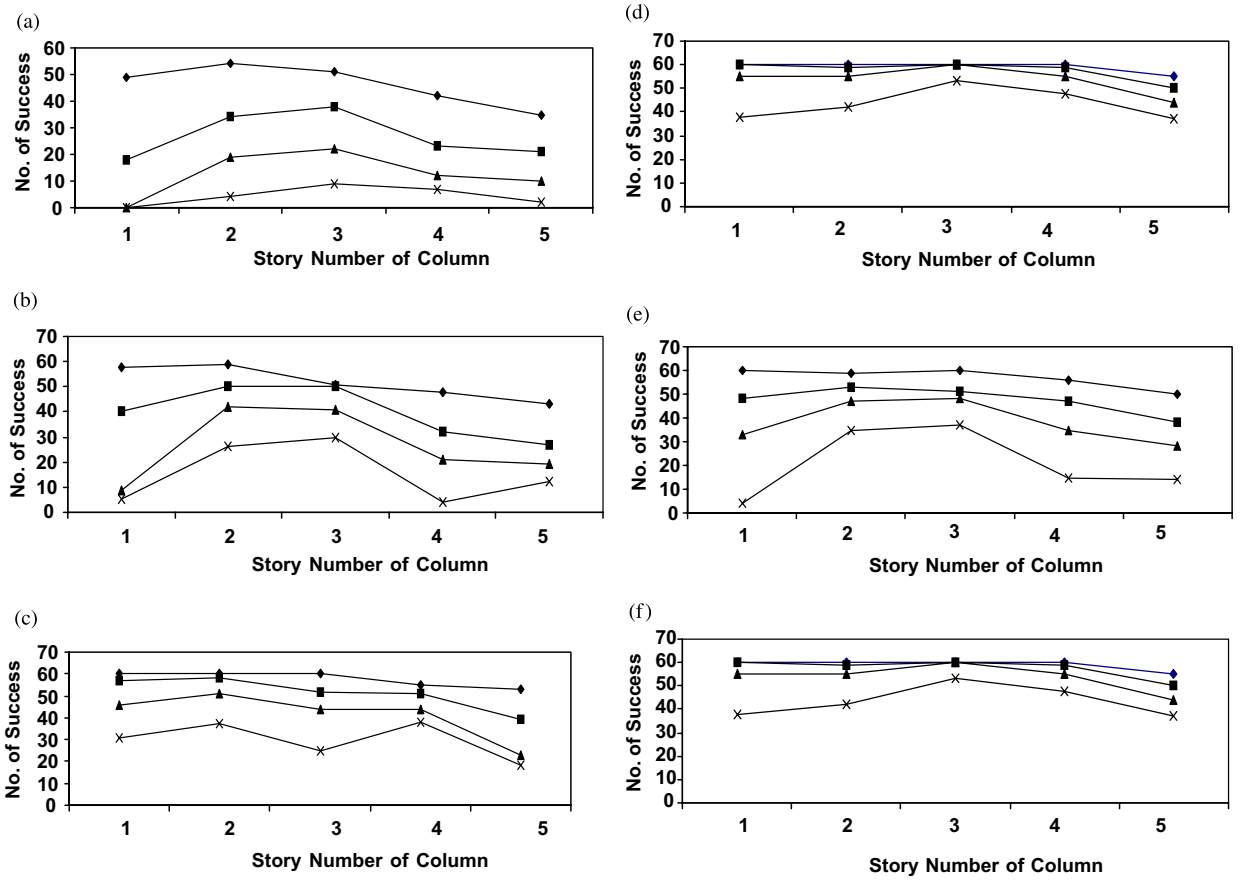

Fig. 6. Prediction of damage in columns for different values of damage and different number of measurements (Error 1%: —◆—, Error 5%: —■—, Error 10%: —▲—, Error 20%: —×—): (a) Damage value 25% and 6 sensors. (b) Damage value 50% and 6 sensors. (c) Damage value 95% and 6 sensors. (d) Damage value 25% and 8 sensors. (e) Damage value 50% and 8 sensors. (f) Damage value 95% and 8 sensors.

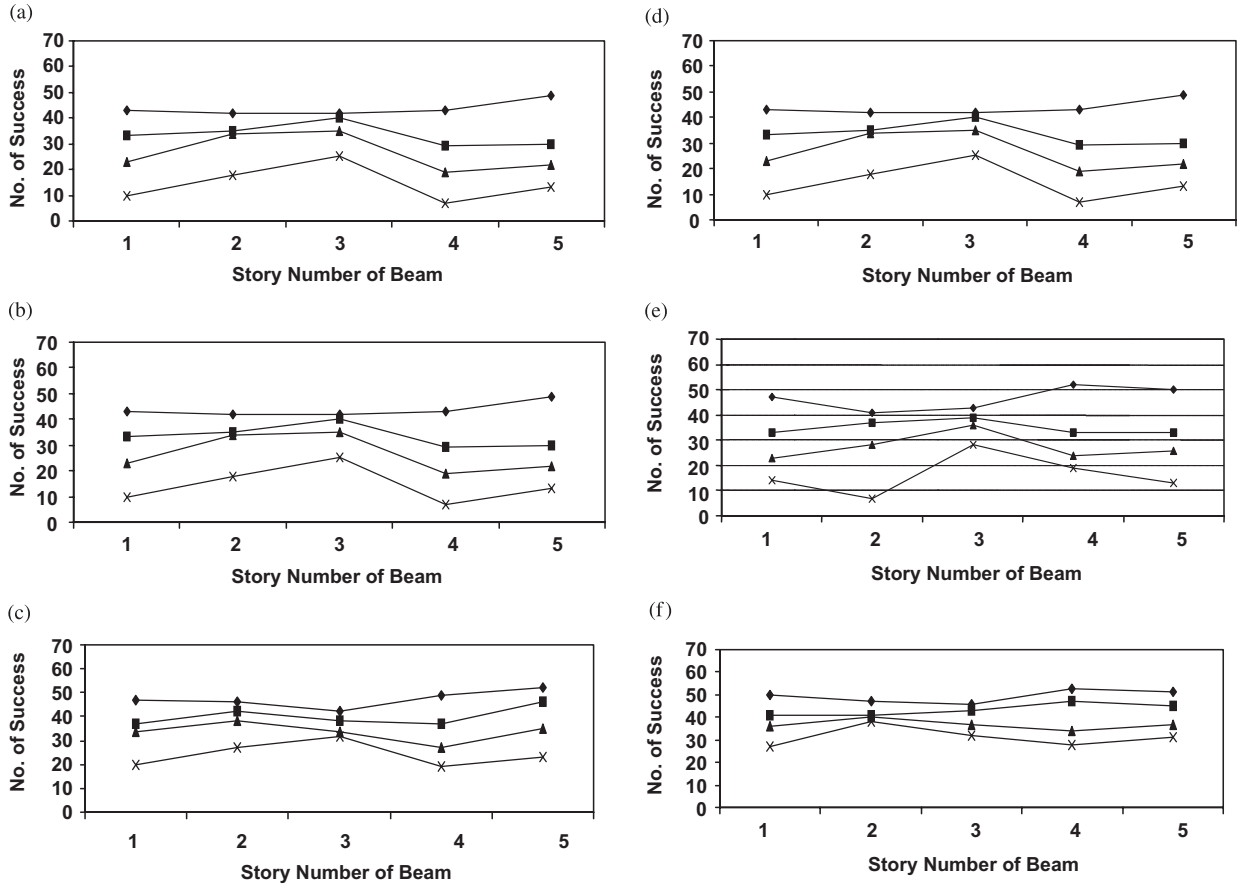

Fig. 7. Prediction of damage in beams for different values of damage and different number of measurements (Error 1%: —◆—, Error 5%: —■—, Error 10%: —▲—, Error 20%: —×—): (a) Damage value 25% and 6 sensors. (b) Damage value 50% and 6 sensors. (c) Damage value 95% and 6 sensors. (d) Damage value 25% and 8 sensors. (e) Damage value 50% and 8 sensors. (f) Damage value 95% and 8 sensors.

The set of curves presented in Fig. 6 shows the capability of the developed algorithm in detection of damage induced in the columns of the structure.

To explain and evaluate the results, consider Fig. 6 and case (a) that is a third story damaged column. The algorithm successfully predicts the location of damaged element about 51 times out of 60 for 1% of error, 38 times out of 60 for 5% of error, 22 times out of 60 for 10% error and 10 times out of 60 for 20% of error. So, one can observe that by increasing the percentage of error, the number of success in predicting the location of damage decreases. But for a reasonable amount of noise (less than 5%) it behaves acceptably.

Comparing cases (a) and (d) one can notice that by increasing the number of measured data, the behavior of the algorithm improves. But for large values of error (e.g., 20%) the results are in general unreliable.

Similarly, we performed the simulation for damaged beams and bracing elements. The results are shown in Figs. 7 and 8, respectively. The same trends in prediction of damage location are observed.

6. Conclusion

Based on the concepts of constrained eigenstructure assignment a damage detection procedure for 2D structures is presented. The method can be used to develop system health monitoring schemes. The paper has focused on 2D frames and investigated the abilities of the proposed method as structural damage detection

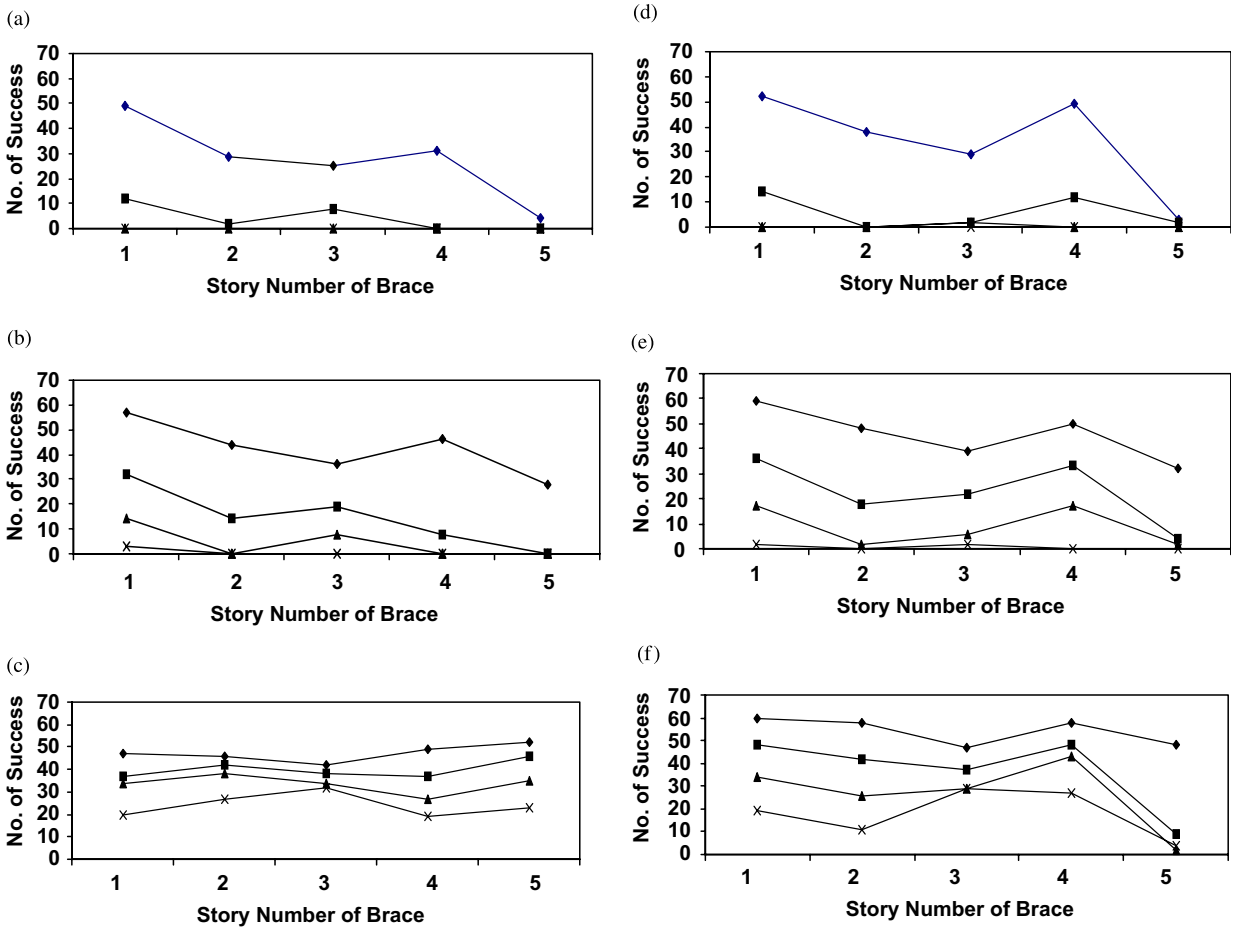

Fig. 8. Prediction of damage in bracing members for different values of damage and different number of measurements (Error 1%: —◆—, Error 5%: —■—, Error 10%: —▲—, Error 20%: —×—): (a) damage value 25% and 6 sensors, (b) damage value 50% and 6 sensors, (c) damage value 95% and 6 sensors, (d) damage value 25% and 8 sensors, (e) damage value 50% and 8 sensors, and (f) damage value 95% and 8 sensors.

and as a system health-monitoring tool. As most health monitoring techniques, this method is case dependent. Its behavior depends on the accuracy of the finite element model of the structure under investigation.

Some of the desirable features of the presented approach are as follows. First, it directly updates the physical properties of structural elements instead of updating matrix of coefficients, which may or may not be physically meaningful. Secondly, it requires only few incompletely measured mode shapes. Finally, it requires neither a solution of algebraic Riccati equation nor any iterative process to converge to a solution. This feature distinguishes the proposed algorithm from the other eigenstructure assignment based damage detection methods.

By observing the trends provided by the shown curves one might deduce the followings results:

(i) Increasing the rate of error in measurements reduces the number of success in predicting the damage location.
(ii) There is a direct relation between the rate of damage and the number of success.
(iii) Damage detection of those elements, which perform a substantial role in the load carrying system of a structure (e.g., story columns) is more achievable than the damage detection of the other elements.
(iv) Increasing the number of sensors (measurements) increases the number of successful predictions.

Finally, the devised approach shows good potential to be used for damage detection of real structures. This method might also be employed for controlling the changes in constitutive parameters of a structure, which is exposed to dangerous event as a real time monitoring devise option.

The effects of sensor location and the type of measured degrees of freedom are two important factors, which cannot be ignored. But, in this study we fixed these two parameters. Besides, the performance of the algorithm for predicting damping changes, which could play a significant role in damage detection process is not studied here.

References

[1] M.S. Agbabian, S.F. Masri, R.K. Miller, T.K. Caughey, System identification approach to detection of structural changes, *Journal of Engineering Mechanics—ASCE* 117 (2) (1991) 370–389.
[2] K.D. Hjelmstad, S.L. Wood, S.J. Clark, Mutual residual energy method for parameter estimation in structures, *Journal of Structural Engineering—ASCE* 118 (1) (1992) 223–242.
[3] K.D. Hjelmstad, S. Shin, Damage detection and assessment of structures from static response, *Journal of Engineering Mechanics—ASCE* 123 (6) (1997) 568–576.
[4] S.W. Doebling, C.R. Farrar, M.B. Prim, D.W. Shevits, Damage identification and health monitoring of structural and mechanical systems from change in their vibration characteristics: a literature review, Los Alamos National Laboratory Report LA-13070-MS, Los Alamos National Laboratory, Los Alamos, New Mexico, 1996.
[5] H. Sohn, C.R. Farrar, F.M. Hemez, D.D. Shunk, D.W. Stinemutes, B.R. Nadler, A review of structural health monitoring literature:1996–2001, Los Alamos National Laboratory Report-13976-MS, Los Alamos National Laboratory, Los Alamos, New Mexico, 2003.
[6] A. Sharifi, Energy Index Method: A Technique for Structural Damage Identification from Either Static or Modal Response, MSc Thesis, Department of Civil Engineering, Shiraz University, Shiraz, Fars, Iran, 2004.
[7] K.D. Hjelmstad, MO.R. Banan, MA.R. Banan, On building finite element models of structures from modal response, *Earthquake Engineering and Structural Dynamics* 24 (1995) 53–67.
[8] S.W. Smith, C.A. Beattie, Secant method adjustment for structural models, *AIAA Journal* 29 (1) (1995) 419–425.
[9] M. Baruch, I.Y. Bar-Itzhack, Optimal weighted orthogonalization of measured modes, *AIAA Journal* 16 (4) (1978) 346–351.
[10] A.M. Kabe, Stiffness matrix adjustment using mode data, *AIAA Journal* 23 (9) (1985) 1431–1436.
[11] D.C. Kammer, Optimal approximation for residual stiffness in linear system identification, *AIAA Journal* 26 (1) (1988) 104–112.
[12] C. Li, S.W. Smith, Hybrid approach for damage detection in flexible structures, *Journal of Guidance, Control, and Dynamics* 18 (3) (1995) 421–425.
[13] T. Pothisiri, J.D. Hjelmstad, Structural damage detection and assessment from modal response, *Journal of Engineering Mechanics—ASCE* 129 (2) (2003) 135–145.
[14] T.W. Lim, Structural damage detection using constrained eigenstructure assignment, *Journal of Guidance, Control and Dynamics* 18 (3) (1994) 411–418.
[15] D.C. Zimmerman, M. Kaouk, Eigenstructure assignment approach for structural damage detection, *AIAA Journal* 30 (7) (1992) 1848–1855.
[16] D.C. Zimmerman, M. Widengren, Correcting finite element models using a symmetric eigenstructure assignment technique, *AIAA Journal* 28 (9) (1990) 1670–1676.
[17] C. Minas, D.J. Inman, Correcting finite element models with measured modal results using eigenstructure assignment methods, *Proceedings of the Sixth International Modal Analysis Conference*, Kissimmee, FL, US, 1–4 February 1988, pp. 583–587.
[18] A.N. Andry, E.Y. Shapiro, J.C. Chung, Eigenstructure assignment system, *IEEE Transactions on Aerospace and Electronic Systems* AES-19 (5) (1983) 711–729.
[19] K. Kahl, J.S. Sirkis, Damage detection in beam structures using subspace rotation algorithm with strain data, *AIAA Journal* 34 (12) (1996) 2609–2614.
[20] T.W. Lim, T.A.L. Kashangaki, Structural damage detection of space truss structures using best achievable eigenvectors, *AIAA Journal* 32 (5) (1994) 1049–1057.
[21] J. He, Z.-F. Fu, *Modal Analysis*, Butterworth-Heinemann, Woburn, MA, 2001.
[22] M. Geradin, D. Rixen, *Mechanical Vibrations—Theory and Application to Structural Dynamics*, Wiley, Chichester, UK, 1997.
[23] N.M.M. Maia, J.M.M. Silva, *Theoretical and Experimental Modal Analysis*, Research Studies Press, Hertfordshire, UK, 1977.
[24] S.R. Ibrahim, E.C. Mikulcik, A method for direct identification of vibration parameters from free response, *Shock and Vibration Bulletin* 47 (4) (1977) 183–198.
[25] J.N. Juang, R.S. Papa, An eigensystem realization algorithm for modal parameter identification and modal reduction, *Journal of Guidance, Control, and Dynamics* 8 (1985) 620–627.
[26] D.L. Brown, R.J. Allemang, R. Zimmerman, M. Mergeay, Parameter estimation techniques for modal analysis, *Proceedings of the Seventh International Seminar on Modal Analysis*, KatholiekeUniversiteit Leuven, Belgium, 1985.
[27] G.H. James, T.G. Carne, J.P. Lauffer, Sandia National Laboratories, The natural excitation technique (NExT) for modal parameter extraction from operating structures, *Journal of Analytical and Experimental Modal Analysis* 10 (4) (1995) 260–277.

[28] L. Hermans, H. Van der Auweraer, Modal testing and analysis of structures under operational conditions: industrial applications, *Mechanical Systems and Signal Processing* 13 (2) (1999) 193–216.
[29] E. Parloo, P. Verboven, M. Van Overmeire, Sensitivity-based operational mode shape normalization, *Mechanical Systems and Signal Processing* 16 (5) (2002) 757–767.
[30] R. Brincker, P. Andersen, A way of getting scaled mode shapes in output only modal testing. *Proceedings of the 21st International Modal Analysis Conference*, Kissimmee, FL, February 3–6, 2003.
[31] P. Mohanty, D.J. Rixen, Identification mode shapes and modal frequencies by operational modal analysis in the presence of harmonic excitation, *Experimental Mechanics* 45 (43) (2005) 213–220.